



Published in final edited form as:

*J Biomed Mater Res A*. 2013 January ; 101(1): 123–131. doi:10.1002/jbm.a.34308.

## Preimplantation processing of *ex vivo*-derived vascular biomaterials: Effects on peripheral cell adhesion

Joseph S. Uzarski, Aurore B. Van De Walle, and Peter S. McFetridge

J. Crayton Pruitt Family Department of Biomedical Engineering, University of Florida, 1275 Center Drive, Gainesville, Florida 32611

### Abstract

The use of *ex vivo*-derived scaffolds as vascular conduits has shown to be a clinically valid approach to repair or bypass occluded vessels. Implantation of allogeneic tissue grafts requires careful processing to lower immunogenicity and prevent bacterial infection. However, the mechanical/chemical treatments used to prepare biological scaffolds can result in significant alterations to the native structure and surface chemistry, which can affect *in vivo* performance. Of particular importance for vascular grafts are binding interactions between the implanted biomaterial and host cells from the circulation and adjacent vasculature. Here we present a comparison of four strategies used to decellularize allogeneic human umbilical vein (HUV) scaffolds: ethanol/acetone, sodium chloride, sodium dodecyl sulfate (SDS), or Triton X-100. Scanning electron microscopy revealed that all four techniques achieved removal of native cells from both the luminal and abluminal surfaces of HUV grafts. Platelets and promyelocytic HL-60 cells showed preferential binding on the more loosely structured abluminal surface, although low surface coverage was observed overall by peripheral blood cells. Vascular endothelial cell adhesion was highest on HUV decellularized using ethanol/acetone, and significantly higher than on SDS-processed grafts ( $p = 0.016$ ). Primary cells showed high viability on the luminal surface regardless of decellularization technique (over 95% in all cases). These results demonstrate the critical effects of various chemical processing strategies on the adhesive properties of *ex vivo*-derived vascular grafts. Careful application-specific consideration is warranted when selecting a processing strategy that minimizes innate responses (e.g. thrombosis, inflammation) that are often deleterious to graft survival.

### Keywords

allograft; cell adhesion; decellularization; endothelialization; extracellular matrix

## INTRODUCTION

Cardiovascular disease is the leading cause of death in the United States, accounting for 1 out of 3 deaths in 2008 alone.<sup>1</sup> The lack of viable autologous vessels in a significant number of patients in need of vascular bypass surgery, a procedure for restoring blood flow, has inspired the search for alternative conduit materials.<sup>2</sup> The disappointing results of many synthetic graft materials in bypass surgeries have led to a shift away from inert biomaterials toward biologically interactive vascular grafts.<sup>3–6</sup>

Despite their limited availability, autografted arterial or venous segments remain the preferred graft choices for vascular bypass surgeries.<sup>7</sup> Natural biological scaffolds, whether autologous or donor-derived, have several features that are favorable for vascular reconstruction.<sup>8</sup> Most importantly, these grafts are composed of proteins, glycosaminoglycans, and other components of the extracellular matrix necessary to support cell adhesion, migration, and proliferation.<sup>9</sup> A significant advantage of biological scaffolds over synthetic polymers is their capacity to be infiltrated and remodeled by host cells through innate catabolic and anabolic processes. Vascular allografts can therefore be repopulated by autologous cells and appropriately adapted to the physiological environment in a site-specific manner.

Immune-mediated rejection is a significant complication with the use of vascular allografts.<sup>10,11</sup> Decellularization of allo-/xenografts is often performed to abate the immune response generated upon implantation of the scaffold by solubilizing and stripping out antigenic cellular components while preserving the native architecture of the extracellular matrix.<sup>12,13</sup> Decellularized donor tissues have shown great promise in applications both as acellular, implantable biomaterials as well as scaffolding material for cell-seeded tissue engineered constructs.<sup>14–20</sup> However, the chemical<sup>21,22</sup> (e.g. organic solvents, detergents, ionic solutions) and mechanical<sup>14,23</sup> (e.g. agitation, sonication, freeze-thaw) methods used to strip immunogenic components out of scaffolds also affect scaffold integrity and therefore the biological responses elicited upon implantation.<sup>13</sup> Because the extracellular matrix composition varies greatly among different tissues, there is no universally applied decellularization protocol.

Due in part to their regular availability, the human umbilical vein (HUV) and arteries have previously been characterized for their ability to function as vascular graft scaffolds.<sup>16,21</sup> Decellularization of the HUV has been described previously by a variety of chemical treatments, including salts, ionic detergents, and a mixture of organic solvents.<sup>16,18,23–25</sup> However, to date, there are no studies specifically addressing how these treatments affect surface interactions at the host-graft interfaces. Adhesive interactions between implanted biomaterials and plasma proteins, circulating/vascular cells, and other components play key roles in the initiation of thrombosis and inflammation, and repopulation/remodeling by native vascular cells.<sup>4,26,27</sup> Minimizing deleterious responses to implantable materials is therefore of critical importance to graft survival.

This study was undertaken for functional assessment of the HUV, an *ex vivo*-derived vascular allograft, after tissue decellularization through various strategies. The HUV was chosen as a target graft due to its increasingly common use as an implantable allogeneic biomaterial in a plethora of applications.<sup>17–19,25,28</sup> Here we characterized the effects of an organic solvent, anionic surfactant, nonionic surfactant, and hypertonic salt solution on the interactive properties of the HUV with peripheral blood and vascular endothelial cells. The objective of this investigation was to comparatively assess surface interactions between processed vascular grafts and cells that play critical roles in tissue performance or graft failure.

## MATERIALS AND METHODS

### Endothelial cell isolation and expansion

Human umbilical cords were obtained from Labor & Delivery at Shands Hospital at the University of Florida (Gainesville, FL) and processed within 12 h of delivery. Human umbilical vein endothelial cells (EC) were isolated from cords using collagenase perfusion, as previously described by Jaffe et al.<sup>29</sup> Media was replenished every 2–3 days with VascuLife basal medium supplemented with VEGF LifeFactors kit (LifeLine Cell

Technologies) and 100 U/mL penicillin/streptomycin (HyClone). After reaching confluence, primary EC were lifted using Accutase with 0.5 mM EDTA (Innovative Cell Technologies) and pooled with primary cells from two other donor cords (for a total of  $n = 3$  donors per lot) to reduce phenotypic variance. Cells were passaged every 2–3 days and used experimentally between P2 and P4.

### HL-60 cell culture

HL-60 promyelocytic leukemia cells transduced with a green fluorescent protein-expressing lentiviral vector were generously provided by Dr. Christopher Cogle (University of Florida Department of Medicine, Gainesville, FL). They were maintained at  $5 \times 10^5 - 2 \times 10^6$  cells/mL in Dulbecco's Modified Eagle Medium supplemented with 20% FBS.

### Platelet isolation

Human venous blood was harvested from healthy adult volunteers after obtaining informed consent. Blood was collected in 10 U of heparin using a 21-gauge needle. Platelet-rich plasma (PRP) was prepared by centrifugation of the blood for 20 min at  $250 \times g$ . The upper platelet-rich layer was obtained and filtered through a Sepharose 2B gel column for acquisition of gel-filtered platelets (GFP).<sup>30</sup> Platelets were fluorescently labeled by adding 10  $\mu M$  of 5-(and-6)-Carboxyfluorescein Diacetate Succinimidyl Ester (CFSE) (Invitrogen).

### Dissection and decellularization of human umbilical veins

Human umbilical veins (HUV) were isolated from the surrounding tissue using an automated dissection procedure that has been described previously.<sup>20</sup> In brief, umbilical cords were rinsed clean and cut into 10 cm sections. After gently massaging out blood clots, cords were threaded through the vein onto a stainless steel mandrel (1/4" OD) and frozen down to  $-80^\circ C$ . After at least 24 h, frozen cords were placed onto a CNC lathe and cut down to a uniform wall thickness of 750  $\mu m$ . Veins were progressively thawed at  $-20^\circ C$  for 2 h,  $4^\circ C$  for 2 h, and then immersed in decellularization solutions at room temperature.

The four decellularization solutions are as follows: a solution of ethanol, acetone, and DI water in a 60:20:20 volumetric ratio (EA); a 2M solution of sodium chloride in DI water (NaCl); 1% (w/v) solution of sodium dodecyl sulfate in DI water (SDS); and a 1% (w/v) solution of Triton X-100 in DI water (TX). Sections were exposed to one of these four solutions under orbital shaking (100 RPM) for 24 h at a 1:20 mass to volume ratio.

After decellularization, sections were rinsed in DI water under orbital shaking for 5 min, 15 min, 40 min, 1 h, 3 h, 12 h, and 24 h. HUV sections were exposed to a solution of deoxyribonuclease I (Sigma-Aldrich) in PBS at a concentration of 70 U/mL under orbital shaking at  $37^\circ C$  for 2 h. Sections were then rinsed in DI water twice for 5 minutes and terminally sterilized in a solution of 0.2% peracetic acid and 4% ethanol in DI water under orbital shaking. Scaffolds were rinsed for 5 min, 15 min, 40 min, and 1 h in DI water, and balanced in PBS (pH 7.40) for 24 h. Scaffolds were stored in PBS at  $4^\circ C$  for a maximum of 2 weeks until use.

### Platelet and leukocyte adhesion assays

Decellularized HUV (dHUV) scaffolds were sliced open axially and cut it into small discs which were placed in the well bottoms of 24-well plates with the seeding surface (luminal or abluminal) facing up. A 400  $\mu L$  volume of gelfiltered platelets (GFP) or HL-60 cells (300,000 cells/mL) was layered on top of the HUV discs. After 2 h of incubation at  $37^\circ C$ , each scaffold was extensively rinsed with PBS. Cells were imaged using a Zeiss AxioImager M2 upright fluorescence microscope with a Zeiss AxioCam Hrm Rev 3 digital camera operated by AxioVision software version 4.8. The amount of platelet or HL-60 cell coverage

were quantified at 7 different locations for each disc and averaged. Platelet distribution was determined using *z*-stack imaging; a series of 2D images at different depths was collected, and cross-sectional images were created by adding the maximal intensity spots of all images together.

### Endothelial cell seeding assay

dHUV discs were prepared as described above and placed in the well bottoms of a 48-well plate with the luminal surface facing up. HUV scaffolds were soaked in Vasculife VEGF culture media with 2% FBS and incubated overnight at 37° C. EC were lifted, counted, and seeded at a density of 10<sup>5</sup> cells/cm<sup>2</sup> (assuming uniform distribution across the well bottom). After 24 h, unattached cells were removed by carefully rinsing in PBS three times before subsequent fixation and processing; rinses were pipetted into the wells along the walls at an angle to avoid shear-mediated denudation of adherent cells. Cells were fixed in 10% neutral-buffered formalin for 10 min, washed three times in PBS, incubated with 4',6-diamidino-2-phenylindole, dihydrochloride (DAPI, 3 nM) for 2 min, and washed again three times with PBS. Nonseeded control scaffolds were similarly processed for each treatment method; no intact or fragmented nuclei were observed on the luminal surface, confirming removal of native endothelial cells. Images were captured as described above. Six fields of view were imaged per scaffold (10× magnification), and the number of cells in each image were counted using NIH Image J software. Attachment (reported as number of cells per surface area) was calculated for five discs per treatment.

### Endothelial cell viability assay

EC monolayers seeded on dHUV scaffolds were assessed for viability using the LIVE/DEAD® Viability/Cytotoxicity Kit \*for mammalian cells (Invitrogen) according to kit instructions. HUVEC were seeded onto dHUV scaffolds at 10<sup>5</sup> cells/cm<sup>2</sup> as described above and allowed to adhere and spread for 24 h. Scaffolds were then rinsed three times in PBS, incubated for 30 min with 2 μm calcein AM (which fluoresces when enzymatically modified by intracellular esterases) and 2 μm ethidium homodimer-1 (an intercalating dye that stains the nuclei in dead or dying cells), rinsed again three times in PBS, and placed onto glass slides for imaging. Images were captured as described above through both the GFP (calcein AM) and DsRed (ethidium) filters to visualize live and dead cells, respectively. Cells were counted as described in the previous section. The percent of viable cells on each scaffold (*n* = 3 per treatment) was calculated using the following formula: % Viability 100 = (#Live cells/surface area)/((#Live cells/surface area)+(#Dead cells/surface area).

### Scanning electron microscopy

HUV samples were placed in the well bottoms of 48-well plates for processing. HUV were fixed in 2.5% glutaraldehyde, washed in PBS, fixed in 1% osmium tetroxide solution, and progressively dehydrated in 25%, 50%, 75%, 85%, 95%, and 3×100% ethanol solutions. Samples were then critical point dried, sputter coated with gold/palladium, and imaged using a Hitachi S-4000 FE-SEM.

### Statistical analysis

Results are presented as mean ± S.E.M. Significance among treatments was determined by one-way ANOVA followed by post-hoc Tukey-Kramer HSD analysis to determine significance between individual means. Student's *t*-test was used to compare HL-60/platelet adhesion on the luminal versus abluminal HUV surface for each treatment group. Asterisks indicate significance at the 0.05 level between individual means (*p* < 0.05).

## RESULTS

### Human umbilical vein isolation and gross morphology after decellularization

Human umbilical vein (HUV) scaffolds were isolated from the surrounding arteries and Wharton's jelly using an automated lathing procedure,<sup>28</sup> resulting in tubular scaffolds 750 microns thick [see Fig. 1(A,B)]. After lathing, HUV were immersed in ethanol/acetone (EA), sodium chloride (NaCl), sodium dodecyl sulfate (SDS), or Triton X-100 (TX) under orbital shaking for 24 h. Decellularized HUV (dHUV) sections derived from the same donor umbilical cord were imaged before subsequent rinse steps for visual comparison of the scaffolds after each treatment [see Fig. 1(C–F)]. Immersion in organic solvents resulted in dehydration and compression of the HUV scaffold [see Fig. 1(C)]. In comparison, treatment with NaCl, SDS, or TX (aqueous solutions) caused progressively increasing swelling of the scaffold [see Fig. 1(D–F)].

### Luminal/abluminal surface characterization

Processed HUV scaffolds were examined using scanning electron microscopy (SEM) to visualize topographical features, surface structure, and global integrity after decellularization. Figure 2 shows representative scanning electron micrographs of both the luminal and abluminal surfaces of HUV subjected to each treatment. All four methods achieved complete removal of the native endothelium, leaving behind the tightly woven basement membrane (BM) structure on the luminal surface [see Fig. 2(A–D)]. Small areas were visible where the BM was partially denuded, exposed the underlying collagen fibrils of the medial layer (see Fig. 2 insets). Larger (5–10  $\mu\text{m}$ ) gaps were observed on NaCl-dHUV and TX-dHUV than on other groups; the BM was left mostly intact in EA-dHUV or SDS-dHUV.

The abluminal surfaces of dHUV, in comparison, showed a much less dense structure, with increased pore sizes present in between loosely woven collagen fibrils [see Fig. 2(E–H)]. Much larger topographical variations were observed on the abluminal dHUV surface than on the luminal surface. No consistent global differences in abluminal microstructure were apparent among the four treatment groups.

### Characterization of platelet adhesion

Platelet adhesion was assessed directly on both the luminal and abluminal surfaces of the HUV after each decellularization method (see Fig. 3). On the luminal surface, the lowest platelet adhesion was observed on EA-dHUV and the highest on NaCl-dHUV. However, no statistically significant differences were observed among decellularization treatments for either surface. Results demonstrated preferential platelet adhesion to the abluminal surface where platelets appeared physically trapped in between collagen fibrils. Overall platelet distribution across a 50  $\mu\text{m}$  scanning depth was observed via z-stack imaging. As shown in Figure 4, platelet adhesion was observed in a continuous line on the luminal surface [see Fig. 4(A–D)], but highly scattered along the 50  $\mu\text{m}$  depth of the abluminal surface [see Fig. 4(E–H)].

### Characterization of leukocyte adhesion

A leukocyte adhesion assay was similarly performed on both the luminal and abluminal surfaces of variously processed HUV grafts (see Fig. 5). Variations in leukocyte adhesion appeared to be highly correlated with surface morphology. Significantly greater adhesion was observed on the abluminal surface of dHUV for all four processing techniques ( $p < 0.05$ ). No statistically significant differences were observed for either surface among decellularization groups.

## HUVEC seeding and culture

Because an intact basement membrane structure was visualized on the processed HUV, we next sought to characterize the ability of endothelial cells to adhere to and repopulate this surface. DAPI nucleic acid staining revealed that EC were able to adhere to the luminal surface of dHUV with a uniform dispersion [see Fig. 6(A–D)]. When HUV were pre-soaked in Vasculife media without FBS, EC were unable to attach (data not shown). EC were able to adhere with high efficiency [over 73% of the cells seeded in all cases, see Fig. 6(E)]. EA-dHUV exhibited the highest EC adhesion ( $101,433 \pm 3498$  cells/cm<sup>2</sup>), which was significantly higher than SDS-dHUV, the treatment which yielded the lowest EC adhesion ( $73,746 \pm 4426$  cells/cm<sup>2</sup>,  $p = 0.016$ ).

## HUVEC viability assay

Viability of re-endothelialized HUV scaffolds was assessed by costaining with calcein AM and ethidium homodimer-1. A high number of live cells was observed on the luminal HUV surface [see Fig. 7(A–D)] with comparatively few dead or dying cells [see Fig. 7(E–H)]. Very high EC viability was observed regardless of decellularization technique [see Fig. 7(I)], with the highest viability on SDS-dHUV ( $99.11 \pm 0.19\%$ ). EC seeded on TX-dHUV, however, demonstrated significantly lower viability ( $96.49 \pm 0.38\%$ ) than on SDS-dHUV ( $99.11 \pm 0.19\%$ ,  $p = 0.001$ ), EA-dHUV ( $98.58 \pm 0.05\%$ ,  $p = 0.004$ ), or NaCl-dHUV ( $98.35 \pm 0.39\%$ ,  $p = 0.008$ ).

## Luminal surface morphology of re-endothelialized HUV

dHUV discs seeded with EC as described above were also processed for S.E.M. analysis. Representative images of reendothelialized dHUV from each treatment group are presented in Figure 8. Twenty-four hours after seeding, monolayers were near confluence, with few gaps present exposing the underlying basement membrane [see Fig. 8(A–D)]. After allowing monolayers to develop further for 7 days, full confluence was observed, and the borders between adjacent cells were more difficult to discern [see Fig. 8(E,F)].

## DISCUSSION

The human umbilical vein (HUV) has been used extensively in vascular bypass surgeries.<sup>31–33</sup> In most cases, however, the graft is chemically fixed using glutaraldehyde before implantation, which masks most antigens and lowers the overall immunogenicity of the scaffold.<sup>31</sup> While glutaraldehyde tanning allows the HUV to be tailored in a site-specific manner (e.g., by fitting the vessel to an appropriate diameter before fixation), crosslinked grafts cannot be infiltrated by host cells or remodeled.<sup>11</sup> This precludes implantation of such grafts in children with congenital cardiovascular defects, as the scaffold cannot truly “grow” over time.

Decellularization, the extraction of immunogenic cellular antigens, is a processing technique that has been explored for allogeneic/xenogeneic organs and tissues as an alternative to glutaraldehyde fixation that allows for extracellular matrix (ECM) remodeling and regeneration.<sup>12</sup> The ideal decellularization process would completely remove or nullify antigens within a graft, while preserving the native extracellular structure, composition, and mechanical properties of the tissue.<sup>12,13</sup> A variety of commonly used decellularizing reagents were chosen for this study, based on their frequent citation in the literature and their differing methods for removal of cellular components. Decellularization of the HUV scaffold with these reagents has been performed previously, and the efficacies of these methods are well-characterized.<sup>16,18,23,24</sup> Here, we compared how these treatments affected extracellular HUV structure and function as they specifically relate to cell adhesion with vascular grafts.

Native structural properties of HUV grafts were affected by these treatments in different ways. Immersion in organic solvents (ethanol/acetone mixture), for example, caused gross dehydration and compression of the scaffold in the radial direction, whereas detergents (SDS/Triton X-100) caused significant swelling of the tissue. Although the variously treated scaffolds normalized in thickness (~ 1 mm thickness) after subsequent rinses, the tissue deformation caused during chemical processing likely resulted in permanent changes to the ECM microstructure. The luminal surface of the HUV is covered by a thin basement membrane, constituted of tightly woven laminin, fibronectin, type IV collagen, and proteoglycans.<sup>8,34</sup> Scanning electron micrographs of the lumen-facing surface showed that scaffolds processed using NaCl or Triton X-100 had large (5–10  $\mu\text{m}$ ) holes in the basement membrane. HUV decellularized using organic solvents appeared slightly more coarse on the luminal surface, indicating mild protein degradation. SDS treatment seemed to best preserve the tightly woven structure of the HUV basement membrane.

Because chemical processing distorts structural tissue features, characterization of functionality is an important precursor to implantation. For allogeneic vascular grafts, no studies to date have specifically addressed how these chemical decellularization strategies affect binding interactions with cells from the peripheral circulation and adjacent vasculature. Binding events at the graft-host interface are critical determining factors in vein graft patency or failure. Thrombosis, intimal hyperplasia, and accelerated atherosclerosis are significant complications in vein allografts, and all are related to excessive adhesion, migration, and proliferation of native cells.<sup>35–37</sup> On the other hand, infiltration by inflammatory cells has been shown to support vascular remodeling in implanted vascular grafts, and tissue ingrowth in aneurysm models.<sup>38,39</sup> A balance therefore exists in producing a scaffold that is resistant to early complications (thrombotic occlusion), yet will still permit appropriate infiltration and ECM remodeling by host cells over time. Here, we sought to characterize cell adhesion at both the endovascular and adventitial surfaces of processed HUV grafts.<sup>4,5,26</sup>

We observed adhesion of both leukocytes and platelets to be significantly higher on the abluminal surface- composed of adventitial connective tissue and glycosaminoglycan-rich Wharton's jelly- relative to the luminal surface.<sup>18,40</sup> Among the four decellularization treatments, there were no significant differences in platelet or leukocyte adhesion with respect to either the luminal or abluminal surfaces. The high variability in platelet coverage may be directly attributable to donor-to-donor variation, as multiple blood draws were necessary. However, the findings in the present study demonstrate the promise of the processed HUV scaffold to resist early platelet adhesion, which is a crucial part of thrombosis. Despite the very high concentration of platelets exposed to the surface, less than 3% of the total surface area was covered for all four treatments compared.

Endothelial cells (EC) showed comparatively higher adhesion on the luminal HUV surface than platelets/leukocytes. Organic solvent-decellularized HUV permitted the highest retention of EC, which was significantly higher than SDS-decellularized HUV. It should be noted that EC adhesion was only observed when decellularized HUV were pre-incubated in medium supplemented with fetal bovine serum (FBS; 2%) overnight. Therefore, it is likely that EC adhesion depended on the selective adsorption of FBS proteins onto the luminal HUV surface, which varied by treatment method. Despite that the basement membrane appeared to be most intact in SDS-dHUV, lowest EC adhesion was observed on this surface. SDS, an anionic detergent, may have induced an overall negative charge to the surface of the HUV, which would repel adsorption of certain protein moieties.<sup>4,41</sup> This would explain the lower observed efficiency of EC adhesion compared to other treatments. Despite initial differences in cell adhesion, scaffolds were lumenally covered in tight monolayers after 7

days culture, indicating that EC could spread, proliferate, and form tight junctions on the processed grafts.

Alteration of the chemical and/or structural properties of the HUV basement membrane also had a significant effect on endothelial cell viability. Scaffolds decellularized using Triton X-100, a nonionic detergent, had more holes visible in the basement membrane region, exposing the underlying collagen fibrils of the medial layer. We observed that endothelial cells seeded onto Triton X-decellularized HUV displayed significantly lower viability when compared with all the other treatment methods. Given the disrupted basement membrane structure and resultant lower viability of endothelial cells observed in the present study, Triton X-100 may not be an optimal decellularization method for the HUV.

## CONCLUSIONS

In this study, we have demonstrated that varying structural alterations induced by decellularizing reagents on *ex vivo*-derived tissue scaffolds result in clinically relevant changes in peripheral/vascular endothelial cell adhesion. Strategies examined here to remove native antigens from HUV allografts (organic solvents, osmotic stress, or ionic/nonionic detergents) were effective, and largely preserved the overall integrity of the HUV scaffold. While it is acknowledged that the bulk mechanical properties of the HUV scaffold are undoubtedly affected in various ways by these chemical treatments, the results presented here underscore that alterations in surface properties influence initial cell adhesion. The basement membrane was mostly retained on the luminal surface with all treatments, though variety in cellular adhesion among treatments indicates that subtle changes in protein structure/surface chemistry existed. Low percent coverage by platelets and leukocytes indicates that these grafts are resistant to excessive early adhesion by inflammatory cells. Processed HUV scaffolds were capable of being repopulated by viable endothelial cells, which attached with high efficiency and grew to confluence on the basement membrane. These results show much promise for further development of the *ex vivo*-derived tissues as implantable vascular biomaterials.

## Acknowledgments

The authors acknowledge Electron Microscopy & Bio-imaging Laboratory at UF for technical assistance with sample processing. They acknowledge Dr. Christopher Cogle and UF Clinical and Translational Science Institute for their assistance with blood draws.

## REFERENCES

1. Roger LV, Go AS, Lloyd-Jones DM, Benjamin EJ, Berry JD, Borden WB, Bravata DM, Dai S, Ford ES, Fox CS, Fullerton HJ, Gillespie C, Hailpern SM, Heit JA, Howard VJ, Kissela BM, Kittner SJ, Lackland DT, Lichtman JH, Lisabeth LD, Makuc DM, Marcus GM, Marelli A, Matchar DB, Moy CS, Mozaffarian D, Mussolino ME, Nichol G, Paynter NP, Soliman EZ, Sorlie PD, Sotoodehnia N, Turan TN, Virani SS, Wong ND, Woo D, Turner MB. Executive summary: Heart disease and stroke statistics--2012 Update: A report from the American Heart Association. *Circulation*. 2012; 125:188–197. [PubMed: 22215894]
2. L'Heureux N, Dusserre N, Marini A, Garrido S, de la Fuente L, McAllister T. Technology insight: the evolution of tissue-engineered vascular grafts—From research to clinical practice. *Nat Clin Pract Cardiovasc Med*. 2007; 4:389–395. [PubMed: 17589429]
3. Twine CP, McLain AD. Graft type for femoro-popliteal bypass surgery. *Cochrane Database Syst Rev*. 2010:CD001487. [PubMed: 20464717]
4. Sarkar S, Sales KM, Hamilton G, Seifalian AM. Addressing thrombogenicity in vascular graft construction. *J Biomed Mater Res B Appl Biomater*. 2007; 82:100–108. [PubMed: 17078085]



5. Kannan RY, Salacinski HJ, Butler PE, Hamilton G, Seifalian AM. Current status of prosthetic bypass grafts: A review. *J Biomed Mater Res B Appl Biomater.* 2005; 74:570–581. [PubMed: 15889440]
6. Johnson WC, Lee KK. A comparative evaluation of polytetrafluoroethylene, umbilical vein, and saphenous vein bypass grafts for femoral-popliteal above-knee revascularization: A prospective randomized Department of Veterans Affairs cooperative study. *J Vasc Surg.* 2000; 32:268–277. [PubMed: 10917986]
7. Sabik JF, Lytle BW, Blackstone EH, Houghtaling PL, Cosgrove DM. Comparison of saphenous vein and internal thoracic artery graft patency by coronary system. *Ann Thorac Surg.* 2005; 79:544–551. discussion 544–551. [PubMed: 15680832]
8. Eble JA, Niland S. The extracellular matrix of blood vessels. *Curr Pharm Des.* 2009; 15:1385–1400. [PubMed: 19355976]
9. Badylak SF, Freytes DO, Gilbert TW. Extracellular matrix as a biological scaffold material: Structure and function. *Acta Biomater.* 2009; 5:1–13. [PubMed: 18938117]
10. Randon C, Jacobs B, De Ryck F, Beele H, Vermassen F. Fifteen years of infrapopliteal arterial reconstructions with cryopreserved venous allografts for limb salvage. *J Vasc Surg.* 2010; 51:869–877. [PubMed: 20347683]
11. Moriyama S, Utoh J, Sun LB, Tagami H, Okamoto K, Kunitomo R, Kitamura N. Antigenicity of cryopreserved arterial allografts: Comparison with fresh and glutaraldehyde treated grafts. *ASAIO J.* 2001; 47:202–205. [PubMed: 11374757]
12. Gilbert TW, Sellaro TL, Badylak SF. Decellularization of tissues and organs. *Biomaterials.* 2006; 27:3675–3683. [PubMed: 16519932]
13. Crapo PM, Gilbert TW, Badylak SF. An overview of tissue and whole organ decellularization processes. *Biomaterials.* 2011; 32:3233–3243. [PubMed: 21296410]
14. Ott HC, Matthiesen TS, Goh SK, Black LD, Kren SM, Netoff TI, Taylor DA. Perfusion-decellularized matrix: Using nature's platform to engineer a bioartificial heart. *Nat Med.* 2008; 14:213–221. [PubMed: 18193059]
15. Macchiarini P, Jungebluth P, Go T, Asnaghi MA, Rees LE, Cogan TA, Dodson A, Martorell J, Bellini S, Parnigotto PP, Dickinson SC, Hollander AP, Mantero S, Conconi MT, Birchall MA. Clinical transplantation of a tissue-engineered airway. *Lancet.* 2008; 372:2023–2030. [PubMed: 19022496]
16. Daniel J, Abe K, McFetridge PS. Development of the human umbilical vein scaffold for cardiovascular tissue engineering applications. *ASAIO J.* 2005; 51:252–261. [PubMed: 15968956]
17. Abousleiman RI, Reyes Y, McFetridge P, Sikavitsas V. The human umbilical vein: A novel scaffold for musculoskeletal soft tissue regeneration. *Artif Organs.* 2008; 32:735–742. [PubMed: 18684203]
18. Chan RW, Rodriguez ML, McFetridge PS. The human umbilical vein with Wharton's jelly as an allogeneic, acellular construct for vocal fold restoration. *Tissue Eng Part A.* 2009; 15:3537–3546. [PubMed: 19456236]
19. Goktas S, Pierre N, Abe K, Dmytryk J, McFetridge PS. Cellular interactions and biomechanical properties of a unique vascular-derived scaffold for periodontal tissue regeneration. *Tissue Eng Part A.* 2010; 16:769–780. [PubMed: 19778172]
20. Crouzier T, McClendon T, Tosun Z, McFetridge PS. Inverted human umbilical arteries with tunable wall thicknesses for nerve regeneration. *J Biomed Mater Res A.* 2009; 89:818–828. [PubMed: 18615471]
21. Gui L, Muto A, Chan SA, Breuer CK, Niklason LE. Development of decellularized human umbilical arteries as small-diameter vascular grafts. *Tissue Eng Part A.* 2009; 15:2665–2676. [PubMed: 19207043]
22. Lumpkins SB, Pierre N, McFetridge PS. A mechanical evaluation of three decellularization methods in the design of a xenogeneic scaffold for tissue engineering the temporomandibular joint disc. *Acta Biomater.* 2008; 4:808–816. [PubMed: 18314000]
23. Montoya CV, McFetridge PS. Preparation of ex vivo-based biomaterials using convective flow decellularization. *Tissue Eng Part C Methods.* 2009; 15:191–200. [PubMed: 19196128]

24. Tosun Z, Villegas-Montoya C, McFetridge PS. The influence of early-phase remodeling events on the biomechanical properties of engineered vascular tissues. *J Vasc Surg.* 2011; 54:1451–1460. [PubMed: 21872418]
25. Issa RI, Engebretson B, Rustom L, McFetridge PS, Sikavitsas VI. The effect of cell seeding density on the cellular and mechanical properties of a mechanostimulated tissue-engineered tendon. *Tissue Eng Part A.* 2011; 17(11–12):1479–1487. [PubMed: 21275843]
26. Afshar-Kharghan V, Thiagarajan P. Leukocyte adhesion and thrombosis. *Curr Opin Hematol.* 2006; 13:34–39. [PubMed: 16319685]
27. McGuigan AP, Sefton MV. The influence of biomaterials on endothelial cell thrombogenicity. *Biomaterials.* 2007; 28:2547–2571. [PubMed: 17316788]
28. Daniel J, Abe K, McFetridge PS. Development of the human umbilical vein scaffold for cardiovascular tissue engineering applications. *ASAIO J.* 2005; 51:252–261. [PubMed: 15968956]
29. Jaffe EA, Nachman RL, Becker CG, Minick CR. Culture of human endothelial cells derived from umbilical veins. Identification by morphologic and immunologic criteria. *J Clin Invest.* 1973; 52:2745–2756. [PubMed: 4355998]
30. Vollmar B, Slotta JE, Nickels RM, Wenzel E, Menger MD. Comparative analysis of platelet isolation techniques for the in vivo study of the microcirculation. *Microcirculation.* 2003; 10:143–152. [PubMed: 12700583]
31. Dardik H, Wengerter K, Qin F, Pangilinan A, Silvestri F, Wolodiger F, Kahn M, Sussman B, Ibrahim IM. Comparative decades of experience with glutaraldehyde-tanned human umbilical cord vein graft for lower limb revascularization: An analysis of 1275 cases. *J Vasc Surg.* 2002; 35:64–71. [PubMed: 11802134]
32. Dardik H. A 30-year odyssey with the umbilical vein graft. *J Am Coll Surg.* 2006; 203:582–583. [PubMed: 17000406]
33. Neufang A, Espinola-Klein C, Dorweiler B, Messow CM, Schmiedt W, Vahl CF. Femoropopliteal prosthetic bypass with glutaraldehyde stabilized human umbilical vein (HUV). *J Vasc Surg.* 2007; 46:280–288. [PubMed: 17600663]
34. Watson SP. Platelet activation by extracellular matrix proteins in haemostasis and thrombosis. *Curr Pharm Des.* 2009; 15:1358–1372. [PubMed: 19355974]
35. Parang P, Arora R. Coronary vein graft disease: Pathogenesis and prevention. *Can J Cardiol.* 2009; 25:e57–e62. [PubMed: 19214303]
36. Johnson TR, Tomaszewski JE, Carpenter JP. Cellular repopulation of human vein allograft bypass grafts. *J Vasc Surg.* 2000; 31:994–1002. [PubMed: 10805891]
37. Haruguchi H, Teraoka S. Intimal hyperplasia and hemodynamic factors in arterial bypass and arteriovenous grafts: A review. *J Artif Organs.* 2003; 6:227–235. [PubMed: 14691664]
38. Roh JD, Sawh-Martinez R, Brennan MP, Jay SM, Devine L, Rao DA, Yi T, Mirensky TL, Nalbandian A, Udelsman B, Hibino N, Shinoka T, Saltzman WM, Snyder E, Kyriakides TR, Pober JS, Breuer CK. Tissue-engineered vascular grafts transform into mature blood vessels via an inflammation-mediated process of vascular remodeling. *Proc Natl Acad Sci USA.* 2010; 107:4669–4674. [PubMed: 20207947]
39. Hoh BL, Hosaka K, Downes DP, Nowicki KW, Fernandez CE, Batich CD, Scott EW. Monocyte chemotactic protein-1 promotes inflammatory vascular repair of murine carotid aneurysms via a macrophage inflammatory protein-1 $\alpha$  and macrophage inflammatory protein-2-dependent pathway. *Circulation.* 2011; 124:2243–2252. [PubMed: 22007074]
40. Stehbens WE, Wakefield JS, Gilbert-Barness E, Zuccollo JM. Histopathology and ultrastructure of human umbilical blood vessels. *Fetal Pediatr Pathol.* 2005; 24:297–315. [PubMed: 16761560]
41. Gratzner PF, Harrison RD, Woods T. Matrix alteration and not residual sodium dodecyl sulfate cytotoxicity affects the cellular repopulation of a decellularized matrix. *Tissue Eng.* 2006; 12:2975–2983. [PubMed: 17518665]

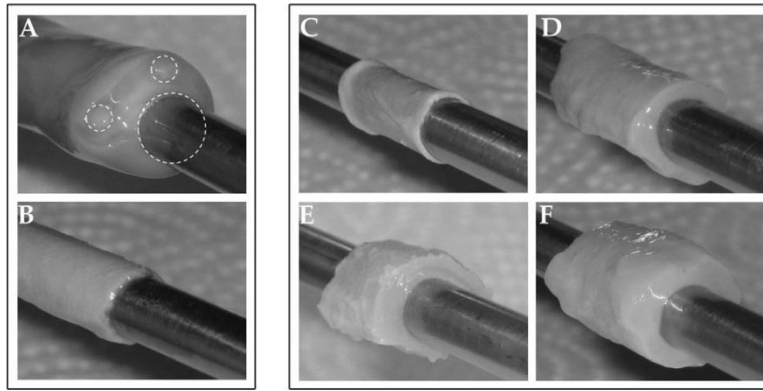


**FIGURE 1.**

Decellularization of human umbilical vein scaffolds. Human umbilical cords were mounted by threading 1/4" steel mandrels through the vein (A), frozen to  $-80^{\circ}\text{C}$ , and lathed down to a thickness of  $750\ \mu\text{m}$  (B). Human umbilical veins (HUV) were then decellularized using one of four chemical treatments: ethanol/acetone (C), sodium chloride (D), sodium dodecyl sulfate (E), or Triton X-100 (F). Shown are representative images of HUV scaffolds immediately following decellularization and before subsequent rinsing/sterilization.

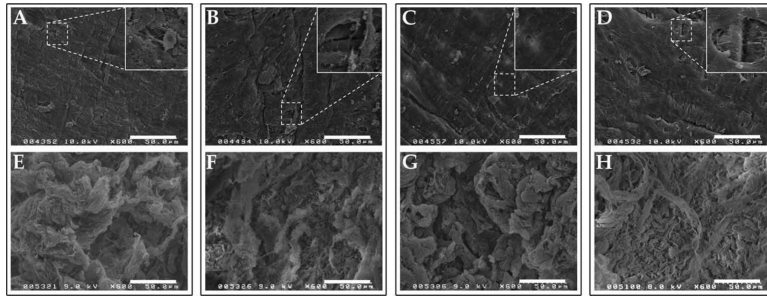


**FIGURE 2.**

Surface characterization of decellularized human umbilical vein scaffolds. Human umbilical veins (HUV) were decellularized using one of four chemical treatments: ethanol/acetone (A,E), sodium chloride (B,F), sodium dodecyl sulfate (C,G), or Triton X-100 (D,H). Shown are representative scanning electron micrographs of the luminal (A–D) and abluminal (E–H) surfaces. All four treatments resulted in complete removal of resident cells from the surfaces of the HUV, while leaving behind the basement membrane (A–D). Small areas where the underlying fibrillar collagen are exposed underneath denuded basement membrane are shown in the insets. Scale bar: 50  $\mu\text{m}$ .

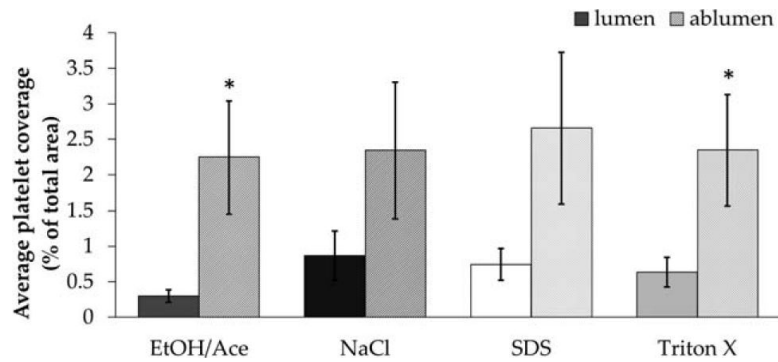


**FIGURE 3.**

Platelet adhesion to decellularized human umbilical vein scaffolds. Human umbilical veins (HUV) were decellularized using one of four chemical treatments: ethanol/acetone (EtOH/Ace), sodium chloride (NaCl), sodium dodecyl sulfate (SDS), or Triton X-100. Percent coverage of the luminal and abluminal surfaces by gel-filtered platelets were quantified and are presented here ( $n = 6$ ). Asterisks indicate significant differences in platelet coverage between the luminal and abluminal surface ( $p < 0.05$ ).

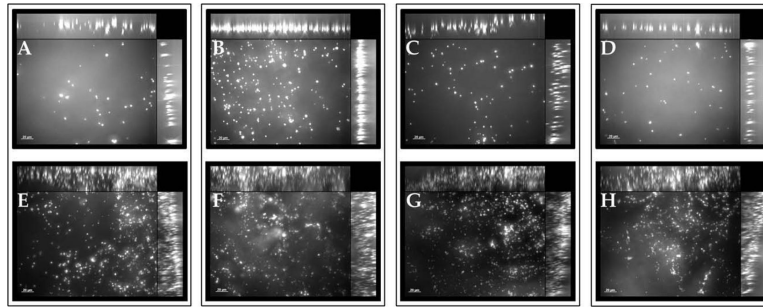


**FIGURE 4.**

Platelet adhesion depth on luminal/abluminal surfaces of decellularized human umbilical vein scaffolds. Human umbilical veins (HUV) were decellularized using one of four chemical treatments: ethanol/acetone (A,E), sodium chloride (B,F), sodium dodecyl sulfate (C,G), or Triton X-100 (D,H). Shown are representative z-stacked images of fluorescently tagged gel-filtered platelets on both the luminal (A–D) and abluminal (E–H) surfaces. Cross-sectional composite images show the distribution of platelets in the z-direction across a 50  $\mu\text{m}$  depth. Scale bar: 20  $\mu\text{m}$ .

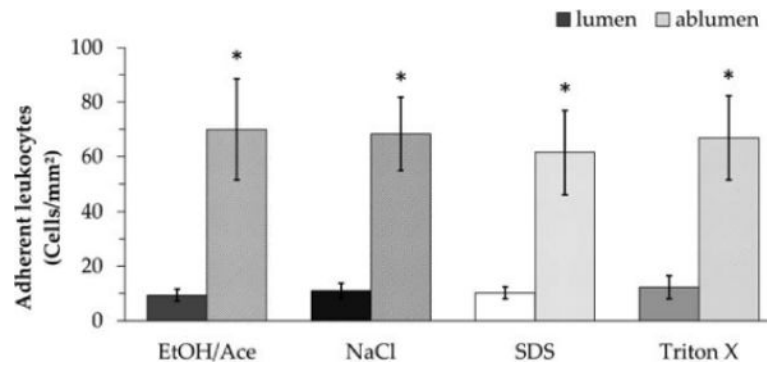


**FIGURE 5.**

Leukocyte adhesion to decellularized human umbilical vein scaffolds. Human umbilical veins (HUV) were decellularized using one of four chemical treatments: ethanol/acetone (EtOH/Ace), sodium chloride (NaCl), sodium dodecyl sulfate (SDS), or Triton X-100. The numbers of adherent HL-60 cells on the luminal and abluminal surfaces were quantified and are presented here as cells per surface area ( $n = 6$ ). Asterisks indicate significant differences in adherent leukocytes between the luminal and abluminal surface ( $p < 0.05$ ).

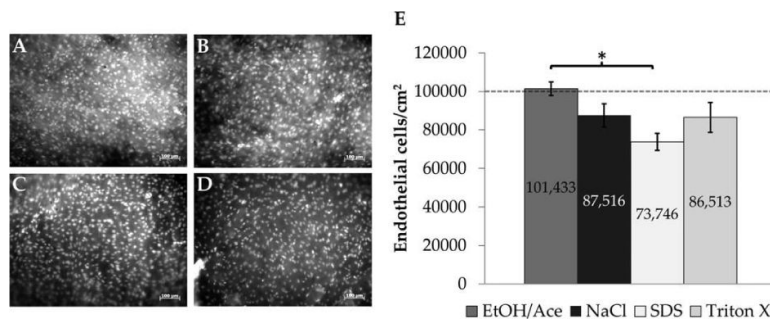


**FIGURE 6.** Endothelial cell adhesion to basement membranes of decellularized human umbilical vein scaffolds. Endothelial cells (EC) were seeded onto the luminal surface of decellularized HUV. Shown are representative images of DAPI-stained EC monolayers after 24 h on HUV scaffolds decellularized using ethanol/acetone (A), sodium chloride (B), sodium dodecyl sulfate (C), or Triton X-100 (D). EC adhesion was quantified on several donor scaffolds ( $n = 5$ ); results are presented per surface area (E). The dashed line indicates the cell seeding density. Asterisk indicates significant differences in mean EC adhesion between treatment groups ( $p < 0.05$ ). Scale bar: 100  $\mu\text{m}$ .



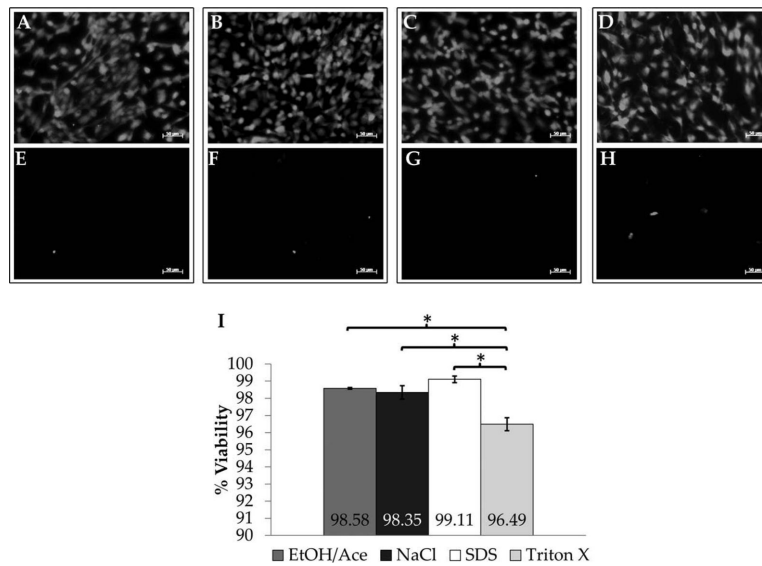


**FIGURE 7.**

Endothelial cell viability on decellularized human umbilical vein scaffolds. Endothelial cells (EC) were seeded onto the luminal surface of decellularized HUV and analyzed using a live/dead viability assay. Shown are representative images of calcein-stained live EC (A–D) and ethidium-stained dead EC (E–H) after 24 h on HUV scaffolds decellularized using ethanol/acetone (A,E), sodium chloride (B,F), sodium dodecyl sulfate (C,G), or Triton X-100 (D,H). EC viability was quantified on several donor scaffolds ( $n 3$ ); results are presented as percent viability (I). Asterisks indicate significant differences in mean EC viability between treatment groups ( $p < 0.05$ ). Scale bar: 50  $\mu\text{m}$ .

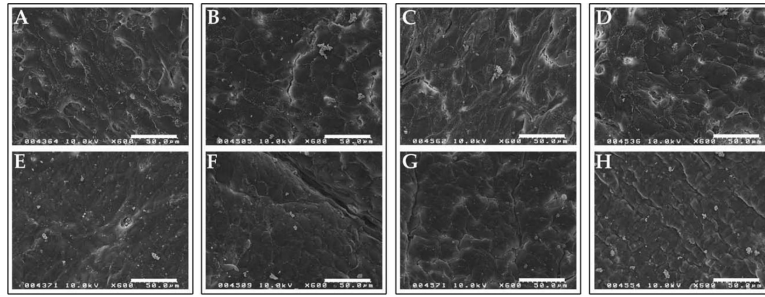


**FIGURE 8.**

Luminal surface morphology of re-endothelialized human umbilical vein scaffolds. Human umbilical veins (HUV) were decellularized using one of four chemical treatments: ethanol/acetone (A,E), sodium chloride (B,F), sodium dodecyl sulfate (C,G), or Triton X-100 (D,H). Primary endothelial cells (EC) were seeded onto the luminal surface of decellularized HUV. Shown are representative scanning electron micrographs of re-endothelialized surfaces after 24 h (A–D) or 7 days (E–H) of culture. Scale bar: 50  $\mu\text{m}$ .